



The contribution of ship emissions to particle concentration downwind of a major shipping route

Bachelor Diploma Work, Summer 2013

Viktor Rusnak, Simon Carreno

Supervisors: Adam Kristensson and Niku Kivekäs

Abstract

Air pollution still poses a serious air quality problem. There are numerous of different sources for air pollution. One of them is ship traffic, which has an effect on human health as well as the climate system. We decided to investigate one of the largest shipping lanes in the North Sea to what extent ships actually contribute to the particle concentrations in inland locations. Both particle number and volume concentrations between 12 and 500 nm in diameter are investigated in a field study in Denmark performed during the first half of 2012. A method has been developed to calculate how ship plumes in the North Sea ship route are transported to the Danish coast line, and to separate the ship plumes from the background. Finally, the particle number and volume contributions from ship traffic were calculated using two different methods which yielded a lower and an upper estimate of the contributions.

The method showed that the ships contributed to between 10% - 21% of the particle number concentration and between 3% - 18% for the volume concentration on average. These results show that ships play a role in atmospheric pollution and risk to affect human health in inland locations. The data analysis also showed that the method to calculate contributions from ship traffic can be used in any environment where ship traffic is one of the major sources of air pollution.

Table of Contents

List of symbols and acronyms	4
1. Introduction.....	5
2. Aerosol particles	5
2.1 Primary and secondary aerosol particles	5
3. Atmospheric processes	7
3.1 New particle formation	7
3.2 Condensation.....	7
3.3 Coagulation.....	7
3.4 Cloud processing	8
3.5 Deposition	9
3.5.1 Dry deposition	9
3.5.2 Wet deposition	10
4. Climate effect	11
4.1 Radiative forcing.....	11
4.2 Direct climate effect	12
4.3 The indirect climate effect	12
5. Health effects	12
6. Particle emissions and the contribution from ship traffic to particle concentrations	13
6.1 Particles from ship emissions	13
6.2 Health effects linked to ship-induced emissions and future projections of ship traffic in the Arctic.....	14
7. Methodology	16
7.1 Field site	16
7.2 Instrumental set-up.....	17
7.3 Trajectory analysis and classification of days.....	19
7.4 Particle concentration	21
7.5 Particle volume concentration analysis.....	24
8. Results	26
8.1 Particle number and background particle number concentrations	26
8.2 Volume concentration.....	29
9. Conclusion and discussion.....	30
Acknowledgements	33
References.....	34

List of symbols and acronyms

SMPS = Scanning Mobility Particle Sizer

VOC = Volatile Organic Compound

IPCC = Intergovernmental Panel on Climate Change

EAA = European Environment Agency

NaCl = Sodium chloride

SO₄ = Sulphate

NO₃ = Nitrate

NH₄ = Ammonium

NO₂ = Nitrogen dioxide

SO₂ = Sulphur dioxide

PM_{2,5} = Particulate matter with a diameter of 2,5 µm or less

PM₁₀ = Particulate matter with a diameter of 10 µm or less

S = *Supersaturation*

p_A = *Partial pressure of a gas*

p_A^S = *Saturation vapor pressure of a gas*

S_{eq} = *Equilibrium vapor pressure*

S_c = *Critical saturation pressure*

d_c = *Critical droplet diameter*

M_w = *Molecular weight of water*

ρ_w = *Density of water*

N_s = *Number of moles of solute in a droplet*

π = *Pi, a mathematical constant*

R = *The ideal gas constant*

T = *Temperature in Kelvin*

Z_p = *Electrical mobility*

D_p = *Particle diameter*

C_C = *Cunningham slip correction factor*

V = *Voltage of the electrode*

L = *Length of the DMA*

e = *Elementary charge*

n = *Number of charges on particle*

η = *Air viscosity*

Q_{sh} = *Sheat flow of the DMA*

Q_a = *Aerosol flow*

Q_s = *Monodisperse particle flow*

1. Introduction

An aerosol is defined as a volume of air which contains both gases and suspended particles. The outdoor air is an aerosol. Aerosol particles can either be in the liquid or solid state, or could even contain a mixture of these phases.

An increase in solar scattering is expected due to the aerosol particles in the atmosphere, either by direct scattering of sunlight, or indirectly by aerosol particles acting as cloud condensation nuclei (CCN). Also, the exposure of the human population to aerosol particles is an important aspect of adverse effects of pollution.

One way that the atmosphere is affected regionally is through pollution caused by ship emissions. Airborne aerosol particles are released from ship chimneys. These particles go through several processes in the atmosphere, and in the end may alter the radiative balance of the earth. A significant amount of the world's petroleum is burned by transports by road, by aviation and at sea. The fuels used to propel ships are rich in sulphur which gives high concentrations of sulphur dioxide, producing sulphuric acid. The sulphuric acid has a low vapor pressure and rapidly condenses on the surface of any airborne particle, or in lack of existing surfaces produces new aerosol particles.

There are not many studies performed that quantify contributions from ship traffic to inland concentrations, or how ship plumes affect the population of aerosol particles relevant for climate change. In this study, we have calculated the contribution of ship emissions along a major ship route in the North Sea to the size-resolved particle number and volume concentrations measured one hour downwind of the ship route. In this way, we can provide data to estimate how particles emitted by ships, influence climate change and human health.

2. Aerosol particles

2.1 Primary and secondary aerosol particles

Aerosol particles emitted directly into the atmosphere from a natural or anthropogenic particle source, are called primary particles. Gaseous emissions can also lead to particle formation in the atmosphere via gas-to-particle conversion processes. These particles, which normally are formed minutes to days after the first gaseous emission, are called secondary particles. Some hot vapor source emissions, e.g. car exhaust emissions, produce particles through gas-to-particle conversion as the exhaust gas is cooled behind the tailpipe of a car. While these emissions are truly secondary by nature, they are still referred to as primary since they are formed within a second after emission.

Other primary particles are biogenic particles and mechanically generated particles. Two examples of biogenic particles are fungal spores and pollen. Particles formed during wave-breaking at sea, sawing of concrete, re-suspended road and soil dust belong to the group of mechanically generated particles.

Generally speaking, the main chemical compounds of the primary particles formed during oil combustion are carbon and sulphur depending on the sulphur content of the fuel. Organic and sulphur compounds can condense in the cooling exhaust and form primary ultrafine particles below 50 nm diameter. The soot particles formed in the engine are around 50-150 nm diameter in size (Kittelson, 1998). In cities or close to highways where most of these particles are emitted, the concentration can reach several tens of thousands of particles per cubic centimeter of air, while the mass concentration can reach hundreds of $\mu\text{g m}^{-3}$. Wood

combustion particles, from forest fires or wood burning in a wood burner, contain approximately the same basic compounds as oil combustion. One of the main differences is that wood combustion generates more organic sugars than oil combustion (Hedberg et al., 2002). In residential areas in northern Sweden, where wood combustion is one of the dominating sources of heating in the winter, mass concentrations might reach several tens of $\mu\text{g m}^{-3}$ (Hedberg et al., 2006).

The wave-breaking process at sea creates gas bubbles at the sea surface. As the interface between the surface and bubble collapses, film and jet drops are created. When these drops are mixed with air, they are dried up and can remain airborne as aerosol particles. The smaller film drop aerosol particles (in the sub-micrometer size range) contain mostly organic matter while the larger jet drops (super-micron size range) contain mainly sea salt (Facchini et al., 2008).

Soil dust particles consist mainly of minerals. These particles are formed by the wind lifting heavier and larger particles ($\sim 100\mu\text{m}$) which lift lighter particles ($\sim 20\mu\text{m}$) from the ground. These smaller and lighter particles can remain suspended in the atmosphere for a longer time compared to the larger ones. This process is called saltation. Locally, during episodes with high wind speed, the mass concentration may be higher than $100 \mu\text{g m}^{-3}$ e.g. in the Sahara (Querol et al., 2009), while over a typical agricultural field in Europe, the mass concentration of soil particles is normally a few $\mu\text{g m}^{-3}$ (Kristensson, 2005).

The road dust particles generated by the abrasion of the asphalt by car tires, contain e.g. sulphur manganese, iron, copper, nickel and zinc, mostly as oxides. The main chemical composition of the particles is almost the same as for the soil dust particles, since both types come from earth crust material (Kristensson, 2011). The concentration in towns could be as high as several hundreds of $\mu\text{g m}^{-3}$ when spring weather allows for accumulated road dust on the asphalt to become airborne (Johansson et al., 2007).

There are two ways in which secondary particles can form. The first is condensation. As gases absorb or condense on existing particles in the atmosphere, these do not create new particles in the air but change the size and composition of the particles. The secondary process of condensation on the other hand gives an increase in particle mass concentration. The second process is called new particle formation, or sometimes nucleation. In this process, new nanometer-sized particles form as several different vapor molecules bundle together (Kulmala et al., 2004). This process can give tens of thousands of new nanometer-sized particles per cubic centimeter over a region larger than 1000 km in the horizontal direction (Hussein et al., 2009).

Volatile organic compounds (VOCs) can be a source for secondary aerosol particles. In addition, inorganic compounds contribute to the mass of condensable matter, e.g. sodium chloride (NaCl), sulphate (SO_4^{2-}), nitrate (NO_3^-) and ammonium (NH_4^+). The highest amounts of ammonium (NH_4) and nitrate (NO_3) concentrations are found near the sources over continental areas while sulphur dioxide (SO_2) concentrations are mostly emitted at sea from ships (Squizzato et al. 2013). Since secondary formation is not only a source of particles in the atmosphere, but also a process, it will be described in more detail in the next chapter.

3. Atmospheric processes

3.1 New particle formation

New particle formation is a secondary aerosol formation process resulting in high concentration of small nano-meter sized aerosol particles. When only gases participate in the formation, it is called homogeneous nucleation (Kulmala et al., 2002). Supersaturation is necessary for homogeneous nucleation, which means that the vapors participating in the formation experience a vapor partial pressure (p_A) above the equilibrium vapor saturation pressure (p_A^S). The saturation vapor pressure indicates when it is possible for a gas to change phase to become a liquid or a solid. Eq. 1 shows how the supersaturation of a gas is calculated:

$$S = \frac{p_A}{p_A^S} \quad (eq. 1)$$

How much a gas needs to be supersaturated before changing phase depends on the type of molecules and the atmospheric conditions such as the pressure and the temperature.

Supersaturation can only occur when $S > 1$. Equation 1 is valid if only one compound is participating in the nucleation, but the concept is the same if the process involves several compounds.

The process of new particle formation, where gases condense on a liquid or a solid cluster, is denoted as heterogenous nucleation (Kulmala et al., 2002). In this process, the cluster becomes an aerosol particle as soon as it is large enough to be stable. Then it will continue to grow at a more or less constant rate through condensation with other vapors (Kulmala et al., 2004).

New particle formation occurs both in the upper troposphere (Benson, et al., 2007) but also in the boundary layer (Kulmala et al., 2004, Dal Maso et al., 2005). The vapors and chemical composition of clusters that participate in the new particle formation is an open issue, and intense research is carried out at the moment to elucidate this matter (Kulmala et al., 2013).

3.2 Condensation

Particle growth in the atmosphere is mainly due to condensational growth caused by absorption of gases by particles. Condensational growth is accompanied by changes in chemical composition of the particles. How fast the growth occurs is given by the condensational growth rate and depends on how fast low vapor pressure gases can condense onto droplets and thereby increase the particle mass and diameter. Particles with diameters 100-1000 nm, belong to the accumulation mode because they accumulate in the atmosphere due to inefficient removal processes, and since condensational growth has a relatively small effect on diameter growth when the particles are already relatively large in size.

3.3 Coagulation

Coagulation is an important physical transformation processes which an aerosol particle can undergo in the atmosphere. Several particles of varying size collide in this process, and form a slightly larger particle. This growth process is however not as important as the condensational growth process. Instead, coagulation is effective in removing particles from the atmosphere since many of the smallest particles in the range of 1- 10nm diameter are removed from the particle population by coagulation to larger particles. The coagulation rate is strongest

between two particles with a large size difference. The probability for two particles of certain sizes to collide with each other can be expressed through the coagulation coefficient. The coefficient depends on the sizes of the two particles, their relative size difference, the properties of the gas (temperature and pressure), and the number concentration of both types of particles (Kulmala et al., 2001).

3.4 Cloud processing

Nucleation scavenging, or cloud droplet activation, is an atmospheric process where a fraction of the aerosol particles become cloud droplets through activation and others remain non-activated in the air. Cloud droplets cannot be formed in the atmosphere through nucleation of water vapor alone. Water vapor needs a pre-existing surface of aerosol particles (cloud condensation nuclei, CCN) to condense on. The fraction of aerosol particles activated to cloud droplets (the scavenging efficiency) is reduced in clouds which are influenced by anthropogenic sources because the amount of fine mode particles (1-1000 nm in diameter) is increased. This results in a smaller fraction of the particles activating into cloud droplets (Seinfeld et al., 2006).

After activation to a cloud droplet has occurred, the droplet will often evaporate and become an aerosol again. This time the particle will end up in a larger size fraction than before the cloud activation since soluble gases and other particles from the atmosphere have been effectively adsorbed by the cloud droplet (Seinfeld et al. 2006).

The ability of a particle to form droplets depends on the required saturation vapor pressure for the particle to activate. The lower the value is, the easier it is to create droplets. Smaller particles require higher saturation. This is because a small particle has a higher curvature than a large particle, and therefore it has a higher saturation vapor pressure at the surface, making it more difficult for water to condense on it compared to a larger particle with a lower saturation vapor pressure.

This curvature effect is called the Kelvin effect and depends on the droplet size. It increases the required supersaturation for a droplet, and is stronger for smaller particles. The Raoult effect, which is the solute effect, decreases the required supersaturation for droplets containing more soluble material. The two terms are

$$A = \frac{4M_w\sigma}{RT\rho_w} \quad (eq. 2)$$

$$B = \frac{6M_wN_s}{\pi\rho_w} \quad (eq. 3)$$

where A is the Kelvin term and B is the Raoult term.

As the droplet grows, the Kelvin effect increases proportionally to 1^{-d} , but the Raoult effect decreases proportionally to 1^{-d^3} . The combination of the Kelvin and the Raoult effects results in the Köhler curve (S_{eq}) representing the equilibrium vapor pressure at the particle surface

$$\ln S_{eq} = \frac{A}{d} - \frac{B}{d^3} \quad (eq. 4)$$

On this curve there is a maximum equilibrium vapor pressure value (S_c) at some droplet diameter (d_c). These are called the critical saturation pressure and critical droplet diameter, respectively. If that critical saturation pressure is exceeded, it becomes energetically favorable for the droplet to grow infinitely as long as there is water vapor available.

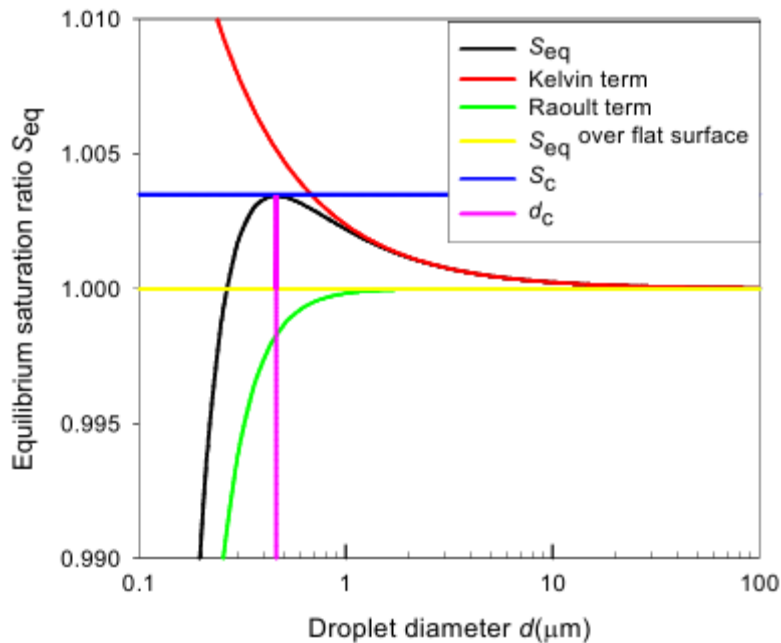


Figure 1. The equilibrium saturation ratio is presented on the y-axis and on the x-axis there is presented the droplet diameter. Also shown are the critical saturation ratio (S_c) and the critical diameter of a droplet (d_c) under pressure (Kivekäs, 2010).

3.5 Deposition

Deposition is an atmospheric process that limits the overall concentration of aerosol particles in the atmosphere. If an aerosol particle deposits on a surface there will be a smaller number concentration of particles in the air. This process can either be dry or wet.

3.5.1 Dry deposition

Dry deposition, which is also known as dry rainfall, occurs when gas or particle substances fall down from the atmosphere onto the ground. The smallest particles do not follow the trajectory of the air molecules exactly. Rather they randomly depart from the air molecule trajectory and therefore have a chance of impacting on a surface. This is called Brownian diffusion. The Brownian diffusion deposition rate increases with decreasing size of the particles. For larger particles, the deposition velocity is high due to sedimentation resulting in fast settling to the ground. Also, impaction and interception are important processes for larger particles. Figure 4 shows different deposition processes. We can see that the deposition is fast for the smallest and the largest particles. It can be seen that for medium sized particles, diameters in the range between 100-1000 nm, the deposition rate is slowest. These particles will accumulate in the atmosphere and grow in size as the particle ages. They belong to the size range called accumulation mode.

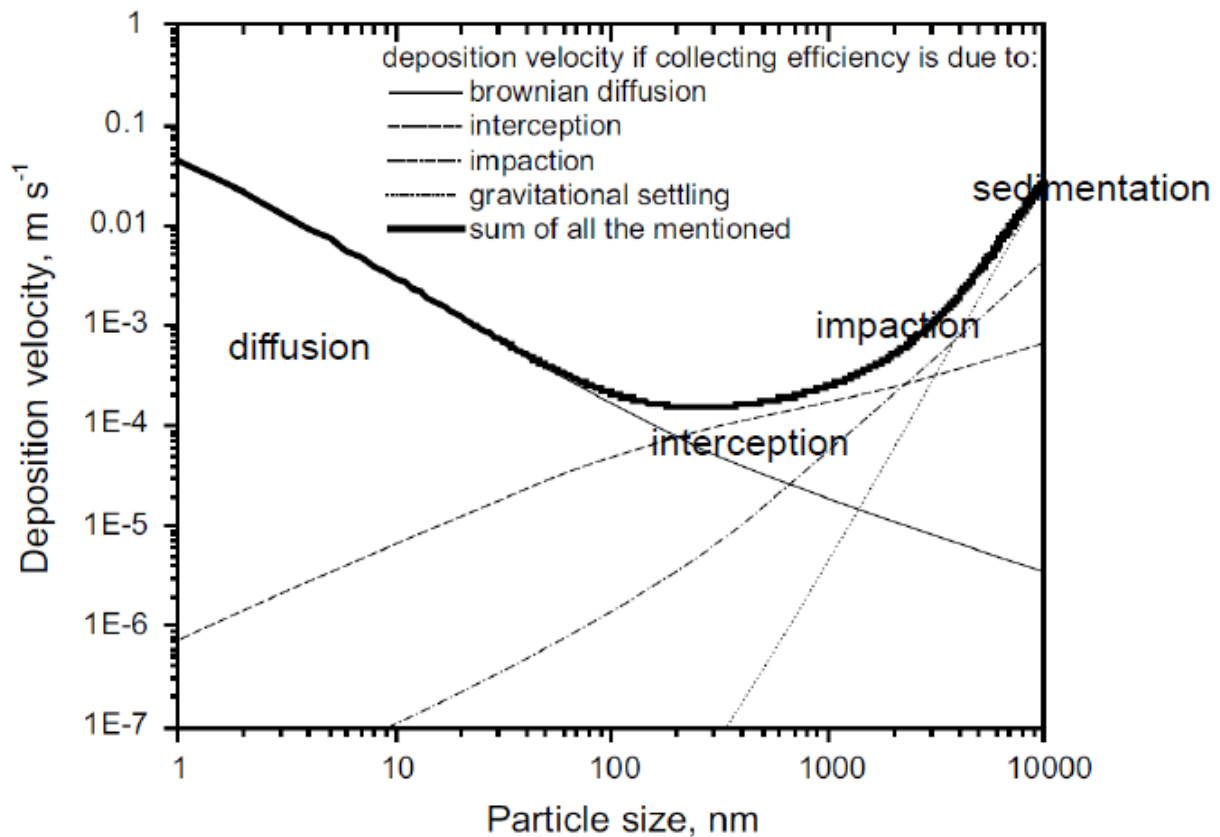


Figure 2. The different deposition processes ranging from small to large particles and slow to fast deposition velocities (Slinn et al., 1982)

3.5.2 Wet deposition

Wet deposition is mainly caused by rain or snowfall. There are basically, two different types of wet deposition and these are:

- Below-cloud scavenging
- In-cloud scavenging.

When aerosol particles collide with falling rain droplets or snowflakes, the droplets merge with the aerosol particles while falling to the ground. This happens mostly below the cloud, and is called below-cloud scavenging. In-cloud scavenging on the other hand refers to when the aerosol particle is being captured by a rain droplet, or when the aerosol particle act as cloud condensation nuclei (CCN), and falls down to the ground at a later step when the droplets have become large enough to become rain droplets.

4. Climate effect

4.1 Radiative forcing

There is a balance between the energy of the incoming solar radiation and that which is re-radiated back to space by the earth. Incoming energy is defined in a positive entity, warming the atmosphere and the earth’s surface, and outgoing energy is defined as a negative entity, cooling the earth. In a stable situation the energy fluxes are in balance. Phenomena that increase or decrease either one of the energy fluxes, thereby shifting the system off balance, are ascribed radiative forcing. This will force the system to warmer or cooler temperature. The radiative forcing is usually compared to the pre-industrial era, assuming that the system was in balance at that time (IPCC, 2007). Figure 3 shows the average present day radiative forcing influenced by different components.

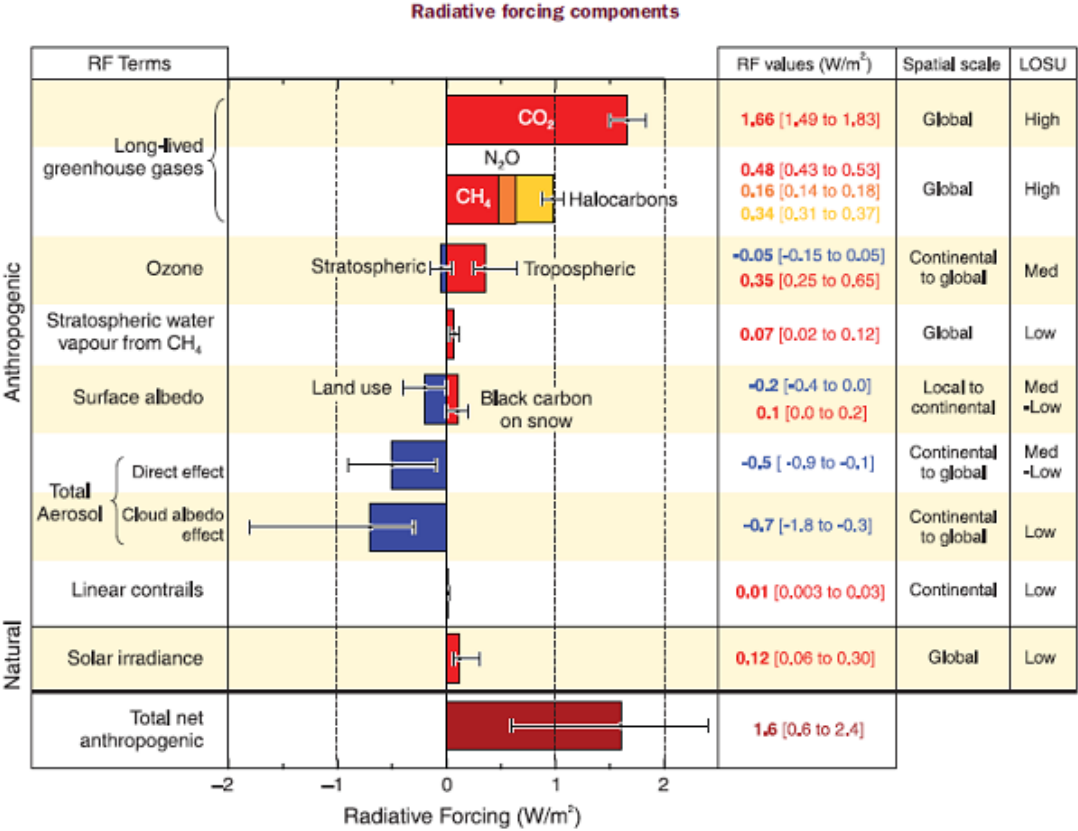


Figure 3. The global average radiative forcing due to different components (IPCC, 2007) in relation to pre-industrial times (1750).

4.2 Direct climate effect

The direct climate effect refers to the change in radiative forcing due to the scattering and absorption of radiation by aerosol particles emitted by human activity. Absorption itself contributes to the reduction of the warming of the earth surface and to an increased warming of the atmospheric layer where the particles are present. Scattering leads to a reduced warming of the atmosphere and earth surface. Particles in the accumulation mode have the largest ability to reflect shortwave sunlight, since the size of the particles causes the internal reflection to create a strong backscattering of sunlight wavelengths.

Fresh soot (black carbon) particles also absorb solar radiation more efficiently than they reflect it, and thereby heat the atmosphere. This is why fresh soot together with other greenhouse gases tends to warm the atmosphere. Additionally, aged soot reflects light to a larger extent than fresh soot. Other types of particles like sulphate aerosol particles or other inorganic particles, as well as organic particles, tend to be more effective at scattering the solar radiation.

4.3 The indirect climate effect

In the first stage of cloud formation, aerosols interact with water vapor and form cloud droplets. The first indirect effect of this is a change in cloud albedo and is named the Twomey effect after its founder (Twomey, 1977). It is the formation of a larger amount of cloud droplets due to a higher concentration of man-made particles, which results in a larger cross sectional area of the cloud than if there were less and larger droplets of the same vapor mass distribution. This effect gives an increased albedo causing a negative radiative forcing.

The second indirect effect is named the Albrecht effect (Albrecht, 1989). With an increase in cloud droplet number concentration due to anthropogenic activities, there will be fewer larger rain drops created and the fog or drizzle will remain for a longer time suspended in the air. Due to the longer lifetime of the clouds, a larger amount of solar energy will be reflected.

Soot particles are hydrophobic and hence not willing to take up water and act as CCN for cloud formation. On the other hand, inorganic particles (for example sulphate particles) are hygroscopic and likely to increase scattering of solar radiation due to the indirect effect.

5. Health effects

Murray et al. (2002) report that anthropogenic aerosol particles cause a premature deaths of 800 000 people annually. The aerosol particles cause the health effects in our respiratory tract. The larger particles that are between 1 and 10 μm in diameters are stopped in the upper respiratory tract, mouth or nose. Particles smaller than 2,5 μm (measured as the mass concentration, $\text{PM}_{2.5}$) are particularly dangerous because of their size which allows them to reach the alveoli. The smallest ultrafine particles (smaller than tens of nanometers) might reach the blood stream and cause cardiovascular and brain diseases (Nemmar et al., 2002). The particles deposited on the lung tissue deep in the lungs are consumed by cells called macrophages. Actuation of macrophages during conditions of oxidative stress, can lead to inflammation in the lungs by the production of reactive oxygen species (ROS) in the body (Kirkham, 2007). Soot particles have an ability to form ROS and these lead to a larger health risk than $\text{PM}_{2.5}$ or PM_{10} (Janssen et al., 2011). The link between cardiovascular diseases and aerosol particles in general is however far from understood (Samoli et al., 2005). Some other severe health reactions might be decreased lung function, irregular heartbeat and in some cases even damage of the nervous system (Oberdorster et al., 2004). For people who already

have respiratory disease, aerosol particle exposure can in the worst case lead to death (Kreyling et al., 2006).

It is beneficial to adapt strategies to decrease inhalation of particles that might lead to unwanted health effects. In connection with these strategies, both positive and negative consequences are probable (Woodcock et al., 2009). Expansion of parks and recreational areas containing vegetation is an example to mitigate an impure atmosphere. Positive consequences might result from planting more trees in rural and urban areas. This is considered to decrease the concentrations of fine particulate matter and ozone (Bowker et al., 2007, Nowak et al., 2006). In addition, tree-shaded areas on buildings would in the long run reduce the amount of electricity used to cool the buildings in the warm seasons, resulting in lower GHG emissions due to reduced carbon emissions from the home appliances (Bolund et al., 1999, McPherson et al., 1997). On the other hand, more tree-shaded areas would result in a darker environment, by preventing sunlight to enter through windows of buildings, thereby increasing the amount of energy used for lighting. Also, more electricity is used for heating the buildings in the cold seasons.

From a health perspective, it might be better to decrease the amount of combustion from machines (e.g. cars) and factories rather than lowering total aerosol emissions, keeping in mind that a larger oxidative stress is caused by metal and soot particles compared to the oxidative stress caused by the total mass (PM_{2.5}) of particles (Genberg, 2013).

6. Particle emissions and the contribution from ship traffic to particle concentrations

6.1 Particles from ship emissions

Mixtures of different particles are released into the atmosphere from combustion in diesel engines which could be on land (e.g. car engines) or in marine environment (e.g. ship engines). Diesel exhaust particles are one of the most common sources of combustion particle. The three most common types are ash and soot particles, sulphuric acid particles and organic hydrocarbons. These are all concentrated in the ultrafine size fraction consisting of both nucleation and Aitken mode particles (10-100nm in diameter). Soot and organic hydrocarbons are the most dominant diesel exhaust products. Some of the particles (belonging to the nucleation mode, <30nm) are formed behind the exhaust pipe in the diluting vapor when they condense in the cooler air. Therefore they cannot be filtered away from the smoke gases.

For emissions from ship diesel engines there is typically a mode of particles found in the size range 20-40 nm as shown in figure 4. Another mode is often found in the size range >100 nm. These particles mainly consist of soot. A study provided by Jonsson et al. (2011) has been conducted outside the Gothenburg harbor comparing emissions from a large number of ships. An example of the difference in particle concentrations for two different ships is shown in figure 4.

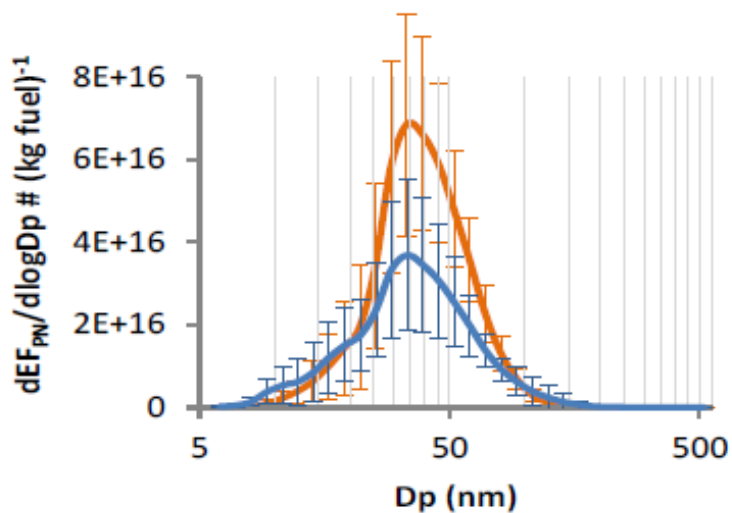


Figure 4. *The number-size distribution and error bars of particles emitted per 1kg of fuel, measured from two different ships and shown here with the blue and orange lines and whiskers (Jonsson et al. 2011).*

Today's ship emissions consisting of various greenhouse gases and other air pollutants, contribute at a global scale to a negative radiative effect, that cool the earth (EEA Technical report, 2013). A study made by the European environment association (EEA) deals with future scenarios for ship emissions. One of these states that by 2020 and onwards the NO_x emissions from ships will be equal to that over the continent and SO_2 emissions in the atmosphere will continue to decrease mainly because of the reduction of sulphur in fuel. The emissions of CO_2 , NO_x , SO_2 and other $\text{PM}_{2.5}$ from ships in Europe, may contribute to as much as 10% - 20% to the worldwide shipping emissions. This tells us what a considerable effect these emissions have globally.

There are options when it comes to reducing sulphur and nitrogen compounds in exhaust emissions. One of these options that has already been taken into account is lowering the sulphuric content in fuel. Another way is to equip engines with filters or similar cleaning systems before the fuel enters the engine (Löndahl et al. 2010).

6.2 Health effects linked to ship-induced emissions and future projections of ship traffic in the Arctic

Figure 5 shows the premature death amongst people who suffered fatal cardiorespiratory complications caused by the ship particle emissions in Europe (Corbett et al., 2007). The author of the study has estimated that 60,000 premature deaths occur globally every year due to $\text{PM}_{2.5}$. Most deaths occur in cities close to the coastlines in Europe, Asia and North America.

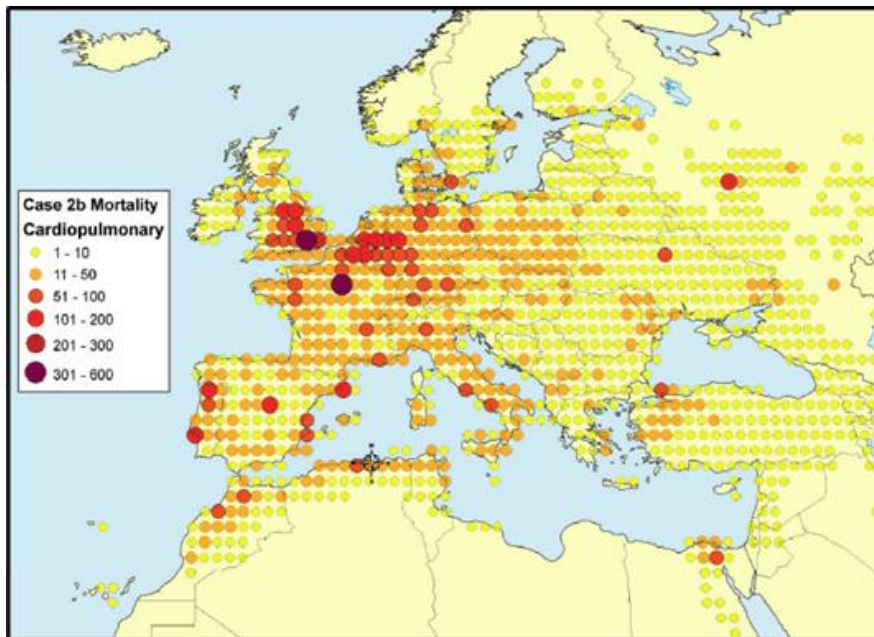


Figure 5. A model of the premature deaths in Europe due to atmospheric contamination from ship emissions (Corbett et al., 2007).

Although the world saw significantly decreased emissions from ship traffic in the 1950's due to a switch to diesel and heavy oil from coal, after some decades emissions again increased (Grübler 1990).

Melting ice in the Arctic is one of many outcomes of increased air pollution and global warming. Smith and Stephenson (2013) predicted that a new shipping route can be used seasonally in the mid 2050's as a result of melting ice, as illustrated in figure 5. The transit times and possibly the cost for shipping would be reduced by using the Arctic transit routes. Even though the new routes might result in shorter transit and thereby potentially reduce greenhouse gas emissions, the reinforced ships would need more power to break through the thick layer of ice resulting in more emissions per time unit. The new shipping route would also bring soot particles right into the middle of the area where they have the largest warming effect (Flanner et al., 2007).

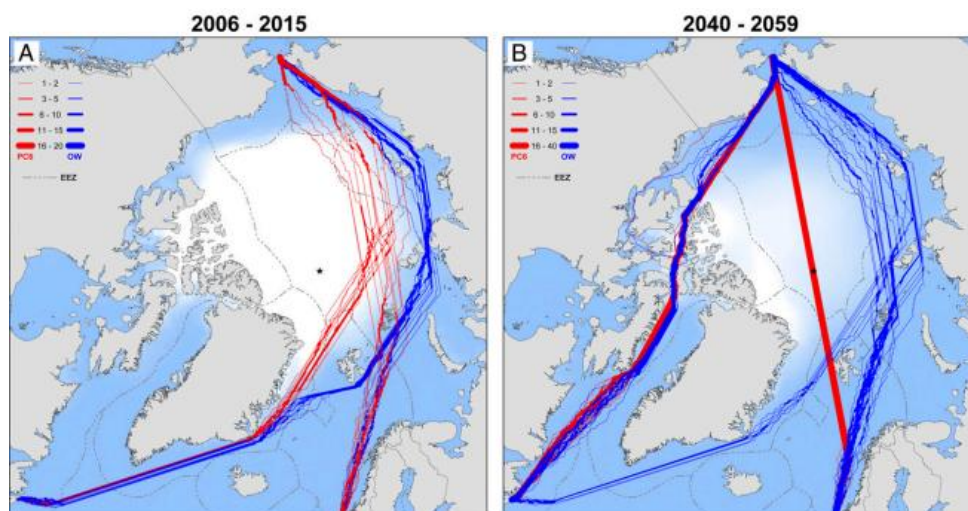


Figure 6. Simulated shipping routes in September through the Arctic in the near future and the mid-21st century, taking into account the changing ice conditions. Blue lines represent open water ships and red lines represent ice reinforced ships (Smith and Stephenson, 2013).

7. Methodology

7.1 Field site

The measurements were performed in Høvsøre (56°26'26''N, 8°09'03''E) at an outdoor wind power research facility at the west coast of Denmark. The measurements at Høvsøre were performed from 09/03/12 to 23/07/12. The instruments were placed ca 1,8 km from the coast line and 15-50 km from one of the most densely trafficked ship lanes in the North Sea. During western and north-western winds, the pollution plume emitted from ships on the shipping lane hit the field site approximately one hour after emission depending on wind speed. The position of the measurement site and the shipping lane are shown in figure 7. From this figure we can see that the westerly winds bring not only particles from the ships on the shipping lane but also from the UK and the oil production areas in the North Sea, that affect the background particle concentration.



Figure 7. The ship lane is located between the yellow lines and the yellow dot shows the location of the field site.

The field site is placed in an open field without any significant industries or plants nearby (figure 8). There is limited activity leading to local emissions of combustion generated particles. Tractors are moving around in the fields during different periods of the year. Working machines used for the wind power station are occasionally driving around the field station. Finally, there is a road along the coast line, but it is not densely trafficked and it is difficult to detect any influence from this road. The activities from the agricultural machinery on the other hand can occasionally lead to an increased concentration of particles at the field site. These elevated concentrations are detected for a few seconds by the instrument. However, they have no significant influence on the average particle concentration at the field site.



Figure 8. *The yellow cross shows where, the experimental instruments are located.*

7.2 Instrumental set-up

The number-size distribution of the aerosols was measured using a scanning mobility particle sizer (SMPS). The size range of the particles, covered by the instrument, was 12-500 nm in diameter. The time resolution is a few seconds, but the data were averaged over 5 minute intervals to get statistically representative values. An SMPS can be seen as an instrument with four main parts; a drier, a bipolar charger, the differential mobility analyser (DMA), and a condensation particle counter (CPC).

Since water and other gases have condensed on the aerosols that we are investigating, the particles are dried before entering the SMPS. This is done by letting the aerosols pass through a naphion type drier where the relative humidity is low, in our case between 5-40%. The losses through this drier have been characterized during the Høvsøre experiments (Lange, Robert, unpublished results, Aarhus University, Aarhus, Denmark, 2013). The losses are highest at 12 nm diameter due to diffusion losses (about 50 %) and approach zero at 200 nm diameter.

A bipolar charger charges a known fraction of the polydisperse aerosols and makes the remaining particles neutral so that measuring the size of the particles will be easier (Zhou, 2001).

The DMA is the core of the instrument. It counts particles of one size at a time. As shown in figure 9, the DMA has the form of a hollow cylinder with a solid electrode at the centre. Between the electrode and the cylinder shell there is a sheath flow of particle-free air that transports the particles which are entering the DMA in the sample flow. If the particles have no charge or are large they follow the sheath flow and outlet exhaust flow in the cylinder. The particles which are too small or are doubly or triply charged are attracted and deposited on the electrode. The particles of the right size-to-charge ratio pass through a small sample exit slit in the DMA as can be seen in figure 9 (Zhou, 2001).

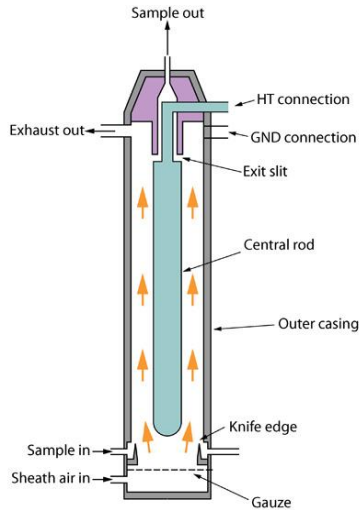


Figure 9. The components and principle of a DMA.

When the monodispersed particles exit the DMA they are counted by the CPC. The particles have to be enlarged by condensation of typically water or butanol. These are counted after condensation because the CPC is not able to count small particles.

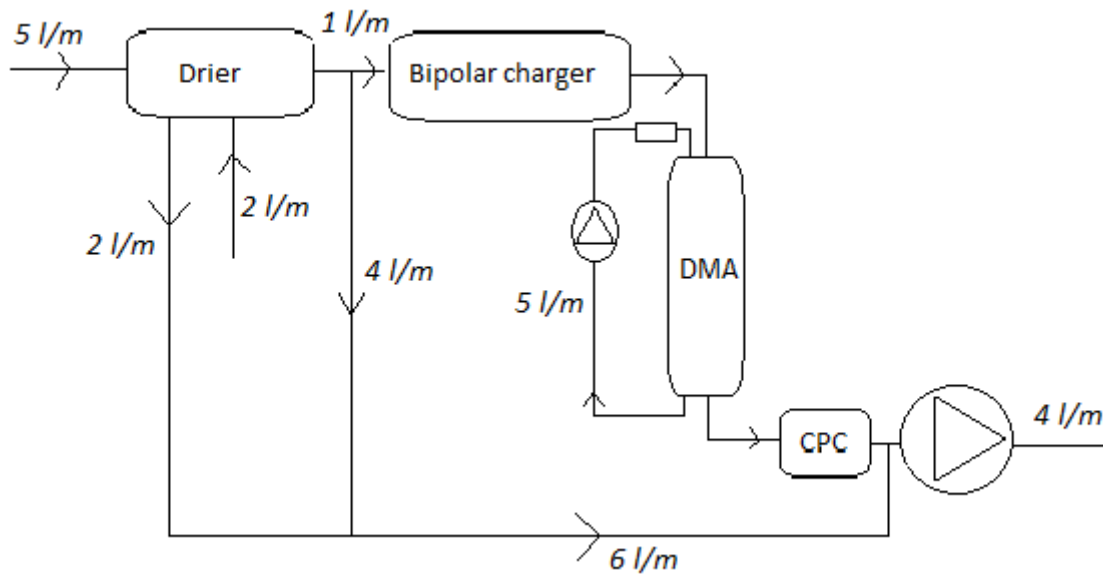


Figure 10. A schematic figure of the SMPS system with the drier. The aerosol flow entering the drier has a flow rate of 5 l/m while the drier itself has a vacuum sheath flow with a flow rate of 2 l/m. After exiting the drier the aerosol flow splits up into two parts, an excess sheath flow with a flow rate of 4 l/m and a new aerosol flow with the flow rate 1 l/m. The DMA has its own sheath flow 5 l/m.

How a charged particle moves in the electric field in the DMA can be deduced through its electrical mobility, Z_p .

$$Z_p = \frac{Q_{sh} \cdot \ln\left(\frac{r_2}{r_1}\right)}{2\pi \cdot V \cdot L} \quad (eq. 5)$$

By relating the mobility to the particle diameter, the following expression is derived:

$$Z_p = \frac{n \cdot e \cdot C_c}{3\pi \cdot \eta \cdot D_p} \quad (eq. 6)$$

By combining eq. 5 and eq. 6 it is possible to calculate the diameter of particles belonging to a certain applied DMA voltage. Hence, in the SMPS, it is possible to measure a size distribution by applying different voltages on the DMA.

Not only particles with a discrete mobility pass through the aerosol exit slit, but also particles with both higher and lower mobility than Z_p have a chance to pass through the slit. The mobility width, ΔZ_p can be written as

$$\Delta Z_p = 2 \cdot \frac{Q_a}{Q_s} \cdot Z_p \quad (eq. 7)$$

where Q_a is the aerosol particles flow into the DMA and Q_s is the monodispersed particle flow through the exit slit. The probability for the particle passing through the slit can then be calculated with the DMA transfer function:

$$TF(Z) = \max\left[0, 1 - \frac{2|Z - Z_p|}{\Delta Z_p}\right] \quad (eq. 8)$$

The probability is highest when the particle has the electrical mobility Z_p .

As explained above the SMPS only counts a fraction of all the particles entering the instrument. Therefore the values from the CPC have to be corrected by taking into account the CPC counting efficiency as a function of size, particle losses in the tubes, drier losses, and the known charge distribution of particles.

7.3 Trajectory analysis and classification of days

It is fundamental for this study to know when the air passed over the ship lanes before arriving at the field station. A model called HYSPLIT (HYbrid Single-Particle Lagrangian Integrated Trajectory) was used to calculate the position of the air mass up to 28 h backwards in time. The calculated trajectories ended 100 m above our measurement station with one hour intervals. The resolution of the backward calculations was also one hour. The model was run for every day during the period 09/03/12 - 23/07/12. The air mass origins were divided into four different categories (table 1).

Table 1. *The classification of the days into different categories.*

Type of day	# of days	Fraction of days in %
Ship days	39	28,5
Other sea days	17	12,4
Inland days	16	11,7
Mixed days	63	46,0
Missing data days	2	1,5
Total days	137	100

Ship days are the days when all the air parcel trajectories passed through a region of the shipping lane between 6°30' E, 56°15' N and 8°00' E, 57°18' N (the black line in figure 11). These were the days used for the analysis. The other sea days are the days when the air mass was transported over sea areas, but not over the part of the shipping lane indicated with the black line. There is some contribution from ships during such days, but since the distance from ship lanes and the field site is relatively large, our analysis is not sufficient for separating the ship plumes from the background. Therefore, these days were not included in the analysis. Inland days are the days when the air masses were coming from inland, mainly from the East. These days are not important for our study since the particles are not coming from the ship lane. When the wind passed over the black line for some fraction of the day, the day was defined as a mixed day. These days are important for our study because some of the particles arrive from the ship lane and therefore do contribute to our results. Figure 11 shows how the typical days for the different categories look like.

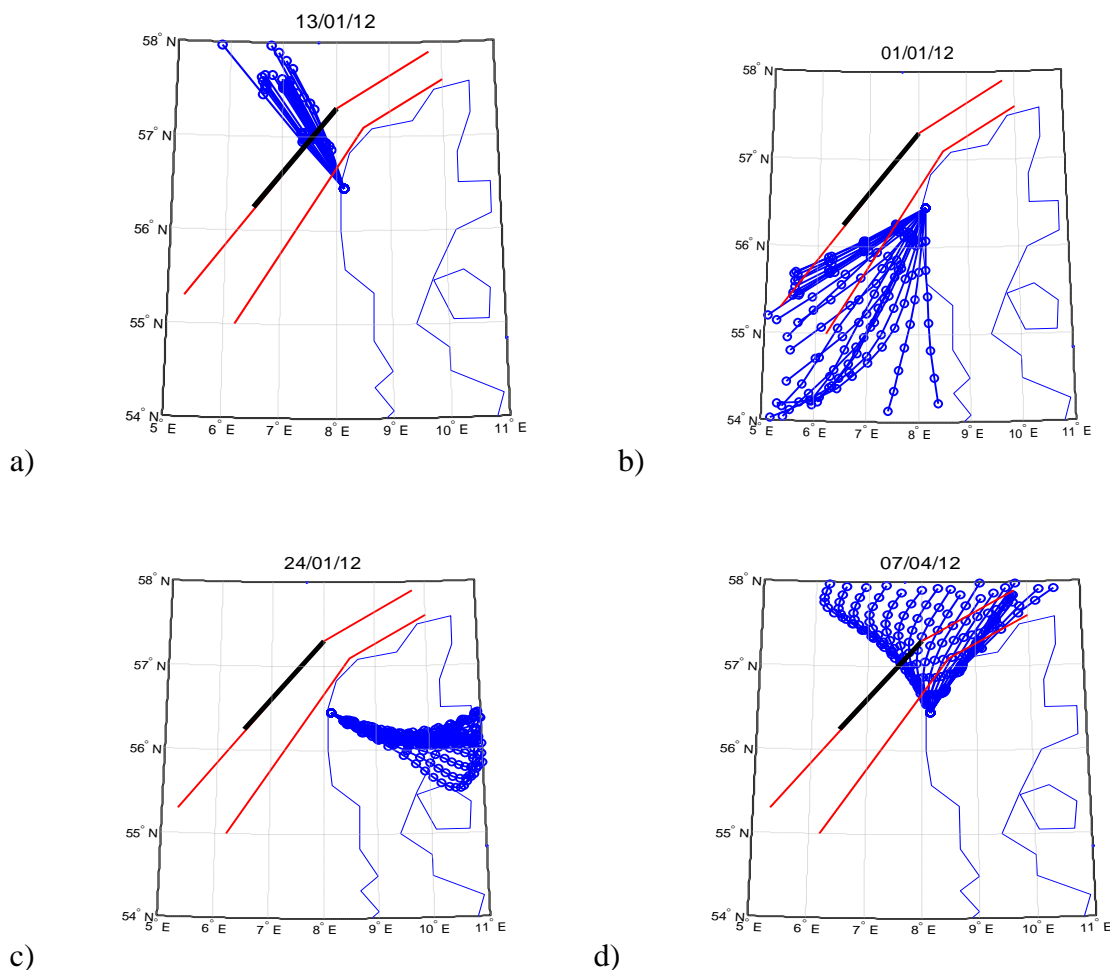


Figure 11. The open circles in the blue lines are the position of the air parcels for each hour before arriving to Høvsøre during a specific day. The black line is the line we used to define ship days and the red lines are the approximate limits of the ship lane. a) A ship day can look like. b) sea day. c) inland day. d) mixed day .

Some of the days have few trajectory data (less than 20 trajectories) and are not used in the analysis, and these are called missing data days.

7.4 Particle concentration

The primary aim was to analyze the number concentration of particles on the ship days. In this way we could examine how large fraction of the particles that arrived to the site from ship plumes and to what extent it was due to background. We defined the background particle number concentration from the daily measurements of the total number of particles as a sliding 25th percentile for a window width of 40 consecutive measurement cycles. These values were used because they seemed to fit best. We also calculated the background particle number concentration for each size class.

Figure 12 shows the total particle number and background concentrations during one day. The difference between these concentrations was assumed to be caused partly by the ship emission and partly by method noise. The particles from the ship plumes at the coast of Høvsøre were determined by subtracting the background particle concentration from the total concentration, leaving only the peaks (figure 13).

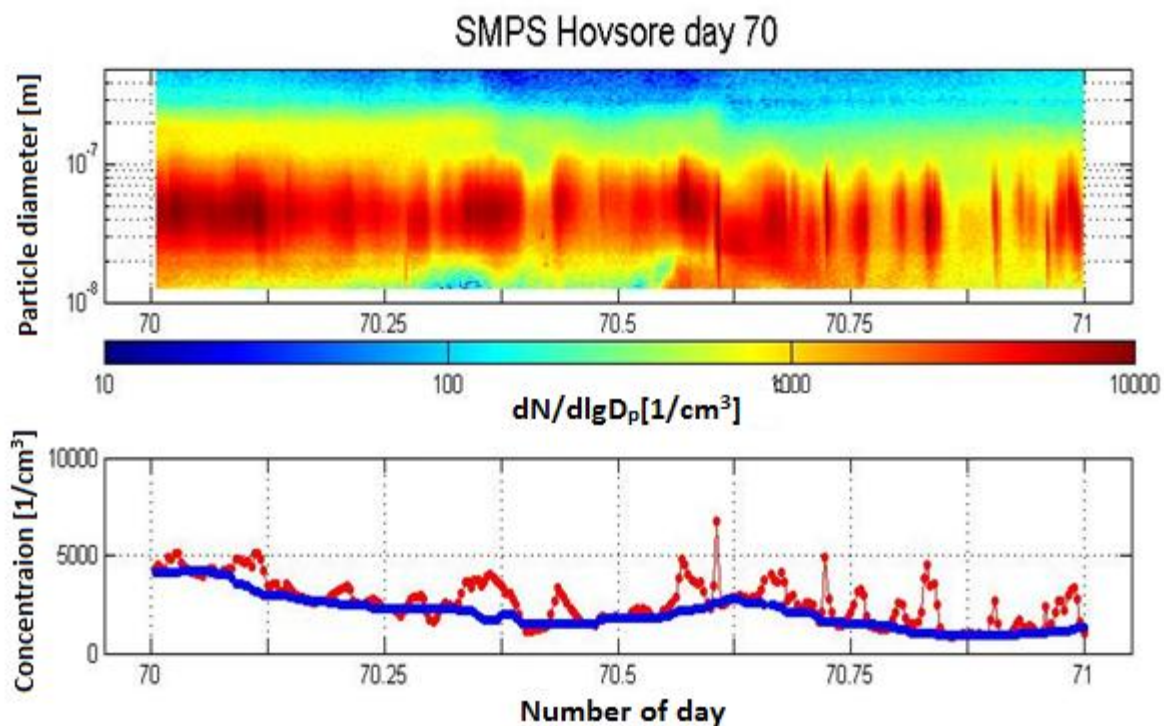


Figure 12. Upper panel: The measured particle size distributions as function of time during the 10th of March 2012. The color represents the particle number concentration in each size class. Lower panel: Total measured particle number concentration (red) and background particle number concentration (blue) as function of time. The total concentration is below the background concentration in some places due to our background is an approximation and negative noise.

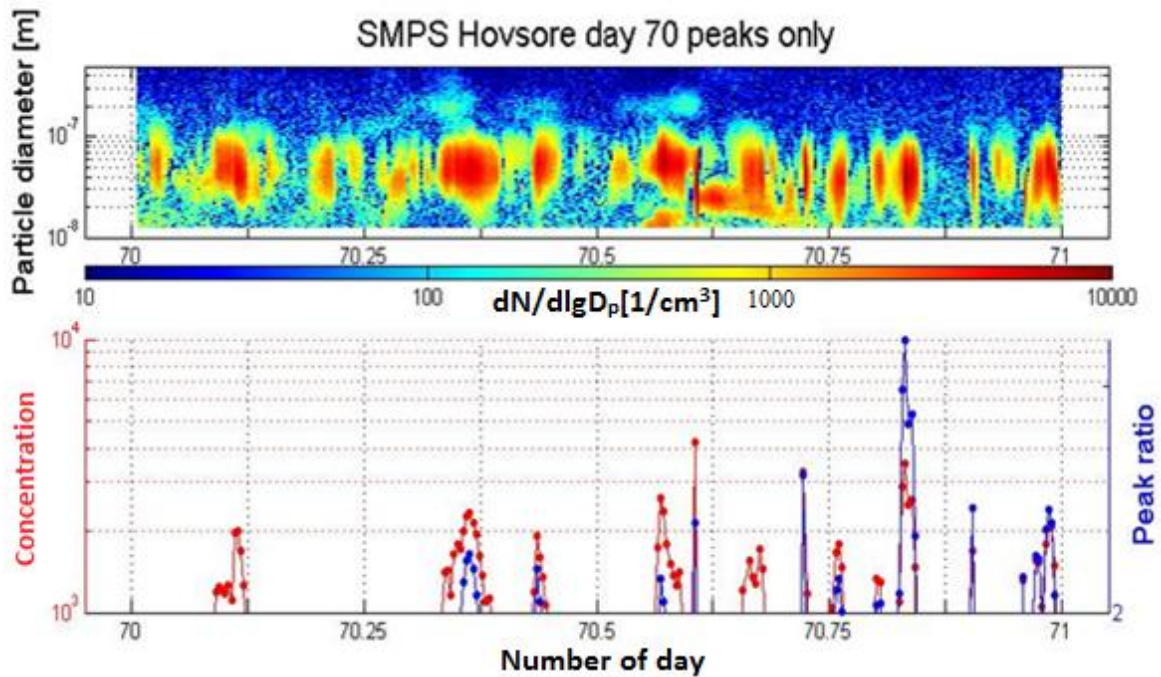


Figure 13. Upper panel: Particle size distributions as function of time as in figure 12, but after subtracting the background. Lower panel: The red line shows the plume particle number concentration and the blue line shows the ratio of total to background particle number concentration.

There were periods when we did not have valid measurements throughout the whole day. Periods when the background concentration shifted rapidly created artificial peaks which looked as if they were coming from a ship. Because we used a sliding 25th percentile of 40 consecutive measurements, the background and the true particle number concentration would in such cases get out of phase. These periods were defined as invalid for our analysis, and were not analyzed.

A plume peak is defined such that either the difference between the peak value and the background value is larger than 1000 particles per cubic centimeter (cm^{-3}) or that the ratio of the total-to-background particle number concentration was larger than 2.

To calculate and further analyze the contributions, the time coordinate was manually taken for every plume peak.

For each plume peak we calculated the following parameters:

- The peak number concentration of the plume particles
- The background particle number concentration
- The total particle number concentration
- The ratio between the total and the background particle number concentration
- Time and duration of the plume
- Total number of plume particles during the plume

Mean values were then calculated not only for each of the days in question but also for all of the days together. We calculated the total particle number concentration in the plumes for each day at a time and the number and time coverage of the plumes for each day. Finally we calculated average values for these.

Finally, we calculated the total daily particle number concentration produced by the ships and the total measured daily particle number concentration during the measurement period. These were used in two different ways to get the contribution of the ship plumes to the total particle number concentration at Høvsøre. The first calculation, which was an overestimate, was made by summing up all the particle number concentration values during the days. This total value included not only the plumes, but also the part of noise where the total particle number concentration was higher than the background values. The other method, which underestimates the results, summed up all the particle number concentration values during periods when the plume- or ratio criteria were met. For the latter calculations, the smaller ship plumes that did not meet the plume criteria were neglected and the outermost parts of the included plumes were not taken into account either. The real values are in between of these estimates. The reason why both estimates were done separately was to be able to define certain limits of our ranges. We also extrapolated the ship plume contribution to the total particle number at Høvsøre for the entire year 2012 assuming that all ship days gave the same relative increase in particle number. We also included the contribution from mixed days and missing data days. This contribution is calculated by multiplying the contribution from ship days with the number of ship days divided by, the total sum of the days (ship days, other sea days and inland days).

7.5 Particle volume concentration analysis

The purpose of this part was to approximate the particle volume contribution from the ships. Almost the same method was used as for calculating the particle number concentration. We calculated the particle volume concentrations and size distribution as if every particle had the form of a sphere, which is an approximation of the real shape. Another approximation was that all particles in a measured size bin had the mean radius of that size bin. For the number concentration this is a good approximation because it is close to the real value but since the volume is the radius raised to the 3rd power, the differences can be significant.

The calculations for the total particle volume were made, and the background contribution was approximated, in the same way as for number concentrations. The figure below shows total volume of the particles during the same day as in our earlier examples. It is worth noticing that most of the particle volume concentration is caused by the particles with largest diameters, even though they were few in number.

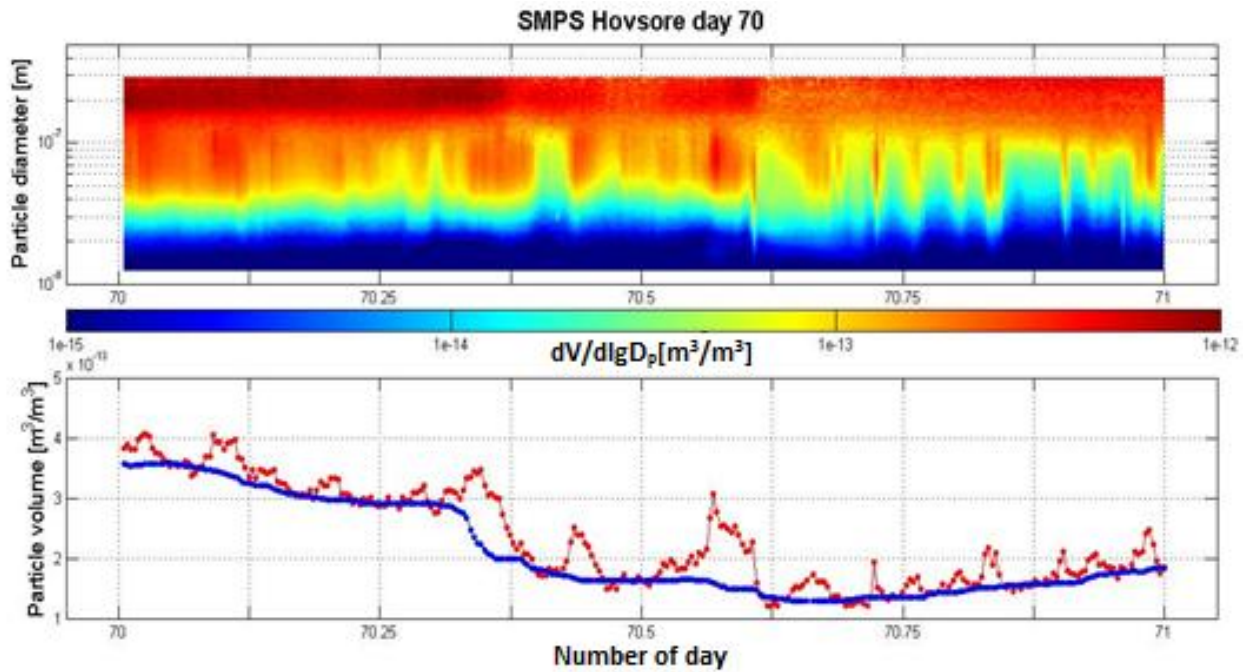


Figure 14. Upper panel: The volume concentration of the particles with different sizes during 10th of March 2012. Lower panel: The total volume concentration of all particles (red line) and the volume concentration of the background particles (blue line)

To see the contribution to the volume concentration from ships the background was subtracted and the ratio between total and background volume concentration was also calculated. The corresponding data is given in figure 15.

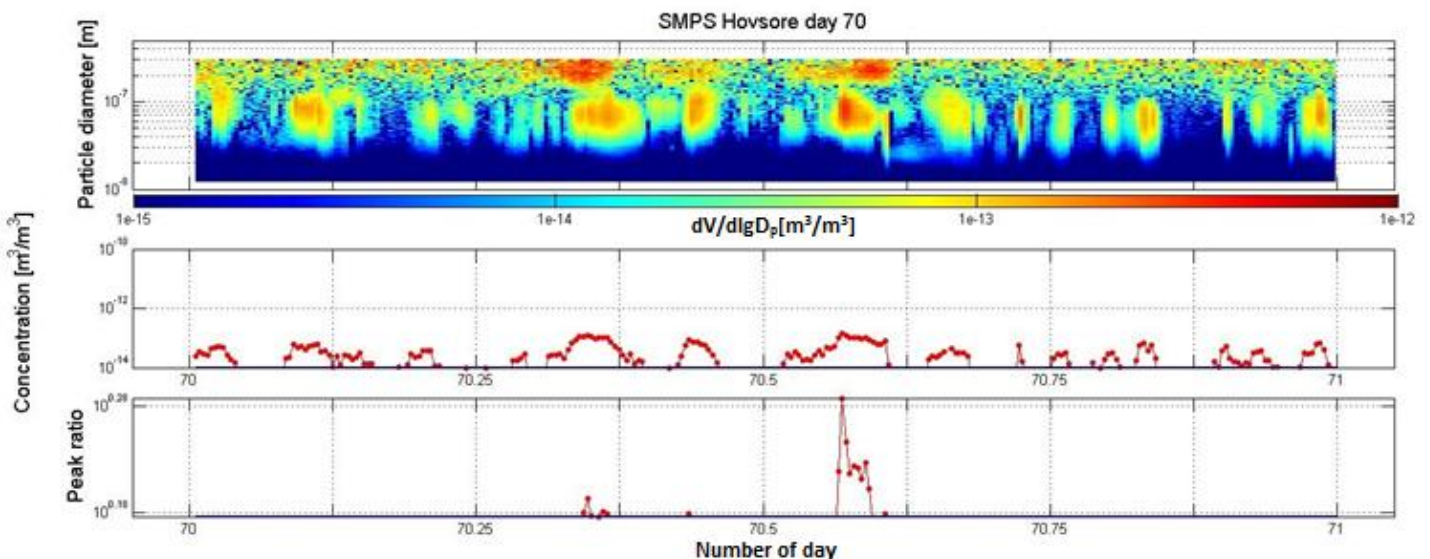


Figure 15. Upper panel: The total volume of the particles (in size range 12-300nm) emitted from ships as a function of time. Middle panel: The total volume concentration from particles emitted by ships. Lower panel: The ratio between the total and background particle volume concentrations.

The volume concentrations of the larger particles (300-500 nm in diameter) could not be correctly analysed because the number of particles was too small. When the particle concentration was low, the noise obtained from the measurements changed the results significantly and the patterns in the graphs are not a good approximation of the real concentrations. This is why graphs were made for two different size ranges: 12-150 nm and 12-300 nm. For a plume to be called a ship plume, the number-based criterion explained in chapter 7.4 had to be met. Note that the definition of a plume is based entirely on the particle number concentration. In order to retrieve the contribution of ship plumes to the total particle volume at Høvsøre an over- and underestimation calculation was done also for the volume concentration as in chapter 7.4

8. Results

8.1 Particle number and background particle number concentrations

The number of detected plumes during each day varied from none to 30. Here it was necessary to note that this was the result for the ship days only. On average we estimated that there were 9.3 plumes per day and these were calculated to cover about 8.6% of the day. Average plume duration was approximately 11 minutes (which covers a little more than two measurements cycles).

The plume peak data remains after subtracting the background data and tells the size range in which the ship-emitted particles were. The size distribution of the particles (figure 16) was interesting and somewhat different compared to a similar work done relatively recently and presented by Jonsson et al. (2011). That study was conducted at the harbor of Gothenburg in Sweden, close to the ships. Our measurements showed average diameter of the plume peak particles to be around 41 nm which, compared to the other work, was a slightly larger. This indicates that the particles must have increased in size by condensational growth or coagulation before they reached land approximately one hour after emissions. Figure 17 shows a histogram for the different peak diameters of the particles.

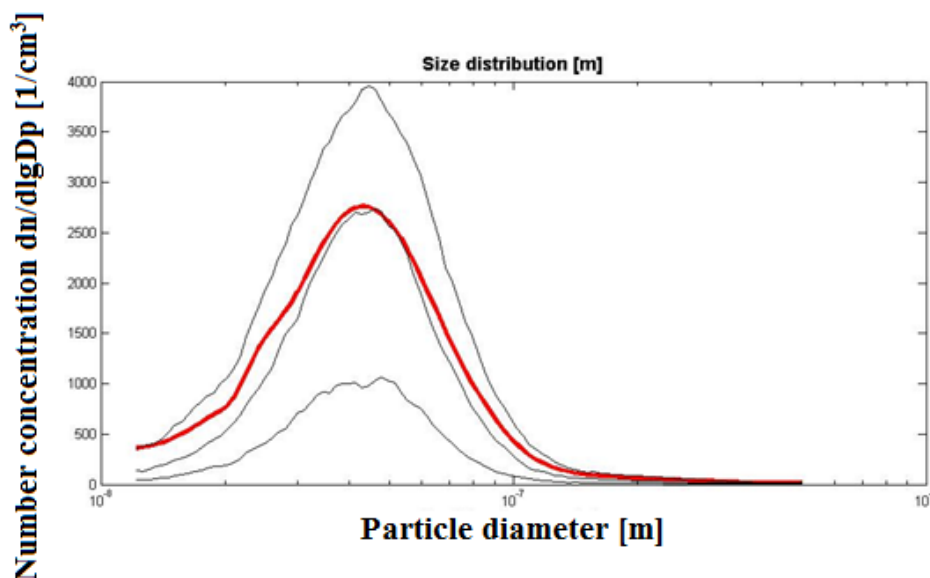


Figure 16. The size distribution for the particles at Høvsøre. The red line shows the average value and the thin black lines show 25%, 50% and 75% values of the size distribution in a logarithmic diameter scale.

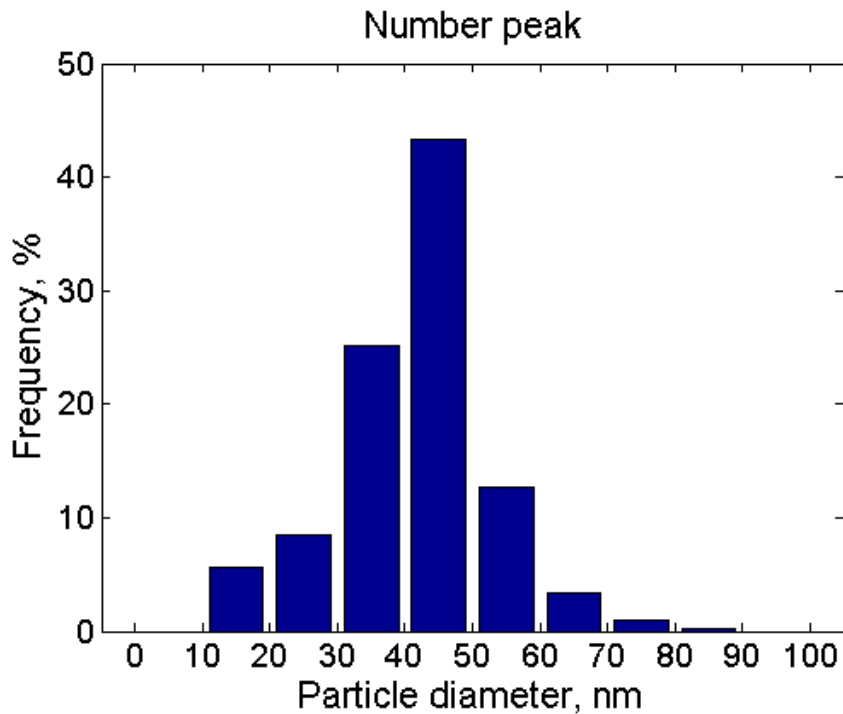


Figure 17. A histogram showing the peak diameter of the particles in the plumes emitted by the ships.

The maximum number concentrations of particles during plumes emitted by ships were typically in the interval 1000-2000 particles / cm³ (figure 18). There were also a number of smaller peaks, but only some of those are included in the analysis (only those that had low enough background concentration to make the total-to-background concentration ratio higher than 2). That explains the lower fractions of peaks in the particle number concentration range below 1000 cm⁻³. Similarly, the peaks with total-to-background particle number concentration ratio below 2 in figure 19 are selected only because of the number of particles in the peak.

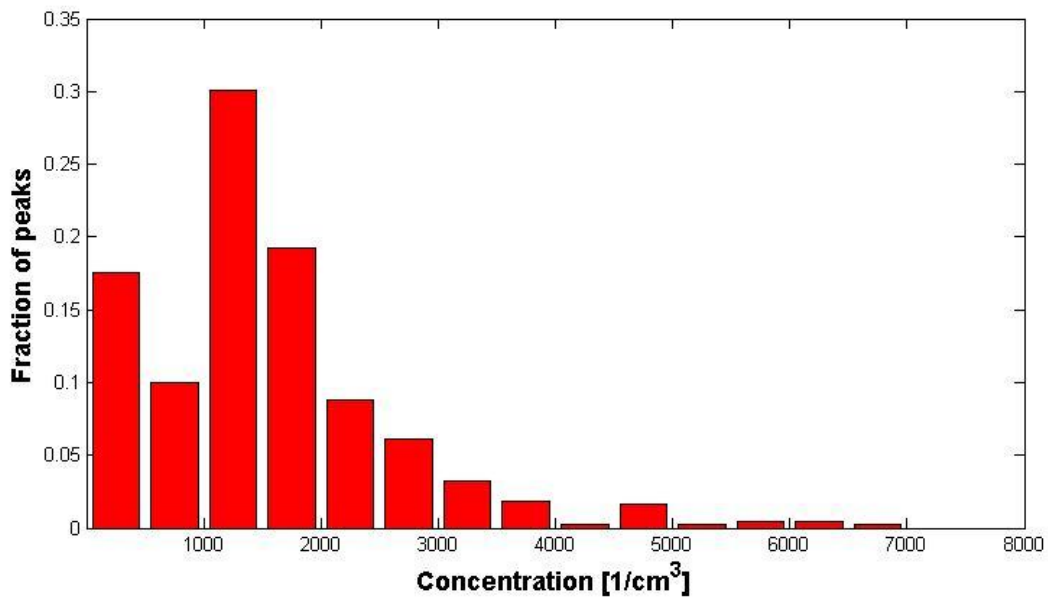


Figure 18. The particle number concentration.

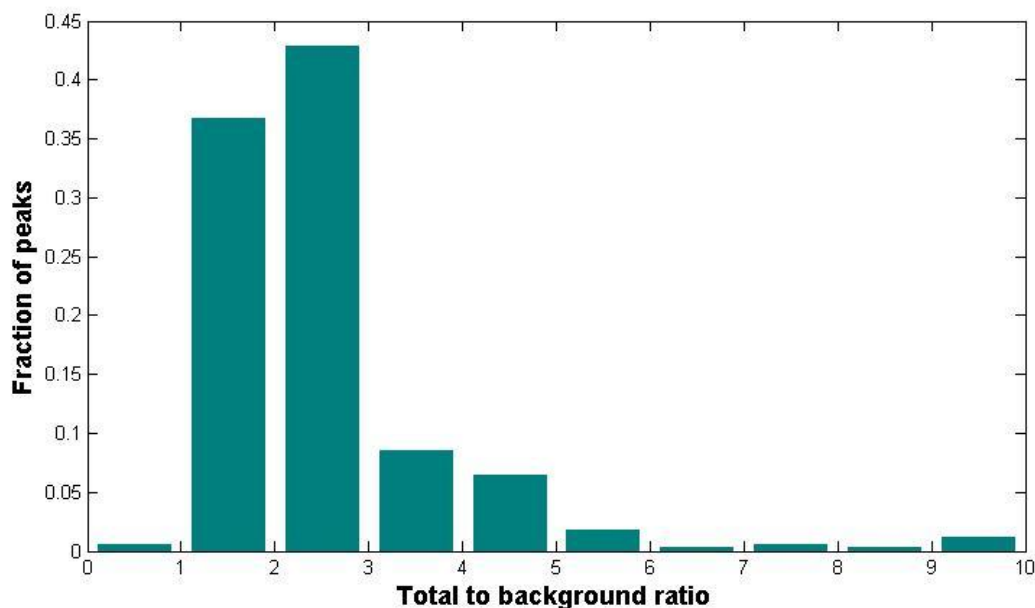


Figure 19. *The ratio between the total particle number concentration and the background particle number concentration.*

An estimate of the contribution of the particle number due to ship emissions over the period for when the ship days dominated was calculated to be 21% with our overestimation method. The underestimation method gave us 10%. As mentioned before, the truth is somewhere in between these estimates (10% - 21%). When calculated for the entire year 2012, the ship contribution to particle number concentrations was 4– 9 %. The results are shown in table 2.

Table 2. *The ship contribution for both volume- and particle number concentration based on the underestimation and overestimation method, respectively.*

	Average ship plume contribution during ship days (%)	Ship plume contribution during entire 2012 (%)
Number concentration	10 – 21	4 – 9
Volume concentration 12-150nm	8 – 18	3 – 8
Volume concentration 12-300nm	3 – 12	1 – 5

8.2 Volume concentration

Since the calculations for the volume concentration are based on the particle number analysis, the results on the number and duration of the peaks are the same as in chapter 8.1. In this subchapter we will instead focus on the volume concentration contributed by ships.

As can be seen in figure 15, a large fraction of the total plume particle volume is in the largest size range (150-300 nm), but the plumes are more visible in the size range 50-150 nm. We can directly notice that the part 150-300 nm is difficult to analyze due to the concentration changes not attributed to ship plumes. This bad quality of the data is due to noise caused by low number of particles measured in this size range. Even though the large particles (150-300 nm) are difficult to analyze, we decided to calculate the volume concentration from this part as well. In figure 15 it appears that only a few ships emit particles in this size range which means that most of the ships have a very low contribution in this size range. If we just look at particles with diameters 150 nm and lower the volume concentration is clearly dominated by the ship plumes. The mode with elevated volume concentrations, appearing in the diameter range 50 to 100 nm, is the equivalent of the maximum number concentration mode in the diameter range from 30 to 60 nm in Figure 16. In figure 19 we can see which particle sizes in the ship plumes contributed most to the volume concentration. We can also see in this figure that the volume concentration increases again in the size range 150-300 nm due to the noise, explained above, and is therefore not a contribution from ships.

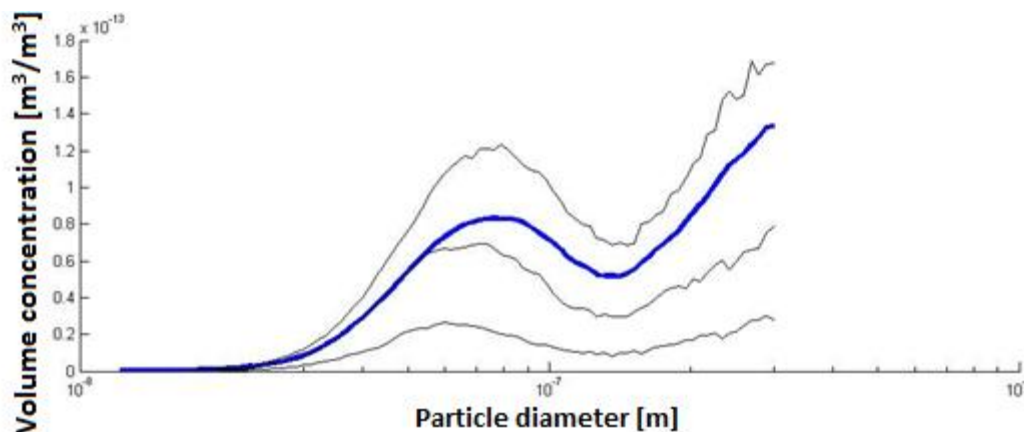


Figure 19. *The size distribution for the volume concentration contributed by ships at Høvsøre in the size range 12-300nm. The blue line shows the average value and the thin lines show 25%, 50% and 75% values of the size distribution in a logarithmic diameter scale.*

Figure 20 shows the peak diameters of the volume-size distribution in two size ranges. The high frequency of the larger particles is also due to noise.

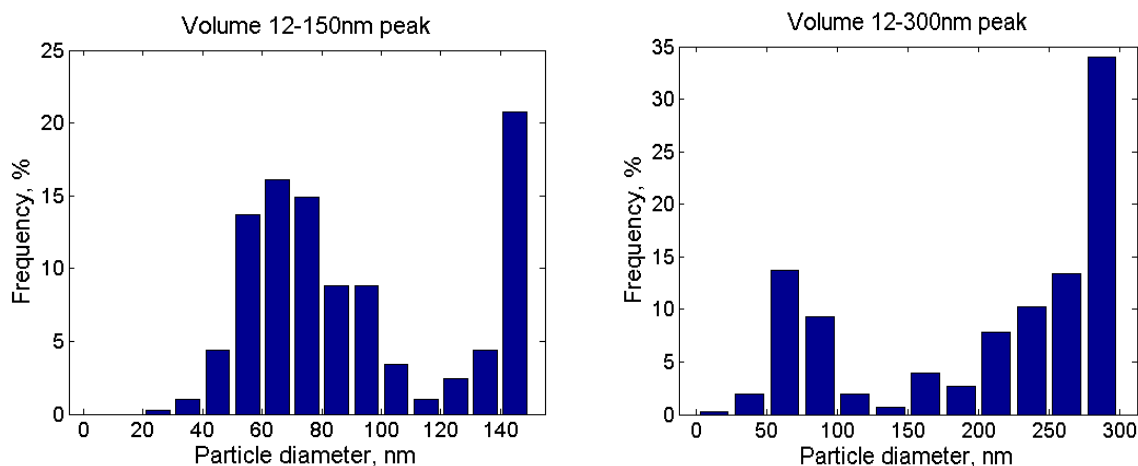


Figure 19. Histograms of the peak diameters in the volume-size distributions of the ship plumes. Left panel: The distribution for particles 12-150nm. Right panel: The distribution for particles 12-300nm.

As explained in chapter 7.5, we calculated the contribution of the ship plumes to the total volume concentration in two different ways; with a method based on an analysis of ship plume peaks (underestimation method), and a method where the background concentration is subtracted from the total concentration (overestimation method). The underestimation method showed that the contribution to volume concentrations from ships are 8% and 3% for the size ranges 12-150 and 12-300 nm, respectively. Using the same method, but calculating for the entire year, we got 1% - 3%. The overestimation method showed that the contribution is 18% and 12% for the size ranges 12-150 and 12-300 nm respectively, and for the entire year it is 5% - 8%. These values are shown in table 2.

9. Conclusion and discussion

An important conclusion is that when a ship passes by Høvsøre, the total particle concentration increases significantly at the measurement site. It is important to note that the analysis focuses only on emissions from the nearest shipping lane and particles from other shipping lanes and industrial sources also arrive at the coast of Høvsøre. These particles are more diluted and contribute to the background particle number concentration, decreasing the relative contribution of emissions from the nearest shipping lane. Therefore we can assume that our results underestimate the total anthropogenic contribution to particle concentrations over this region.

Meteorological conditions such as the height of the planetary boundary layer (PBL) might also affect our results. When the PBL is low the vertical dilution of the particles is reduced. This means that the same amount of particles present in a low PBL results in a high concentration at the Høvsøre station. Rain could also affect the results through the process of wet deposition leading to a reduced particle concentration in the air.

We used a sliding 25th percentile for estimating the background concentrations. This percentile was used because it resulted in a visually good approximation of the background level. If we instead approximated the background concentration with a sliding median, the background particles would reach plume peak concentrations during periods with many plumes over a short time (figure 21). On the other hand, if we had approximated the background with a lower sliding percentile, the background particle concentration would have followed the concentration minima instead of the changing background level, and also produce erroneous values.

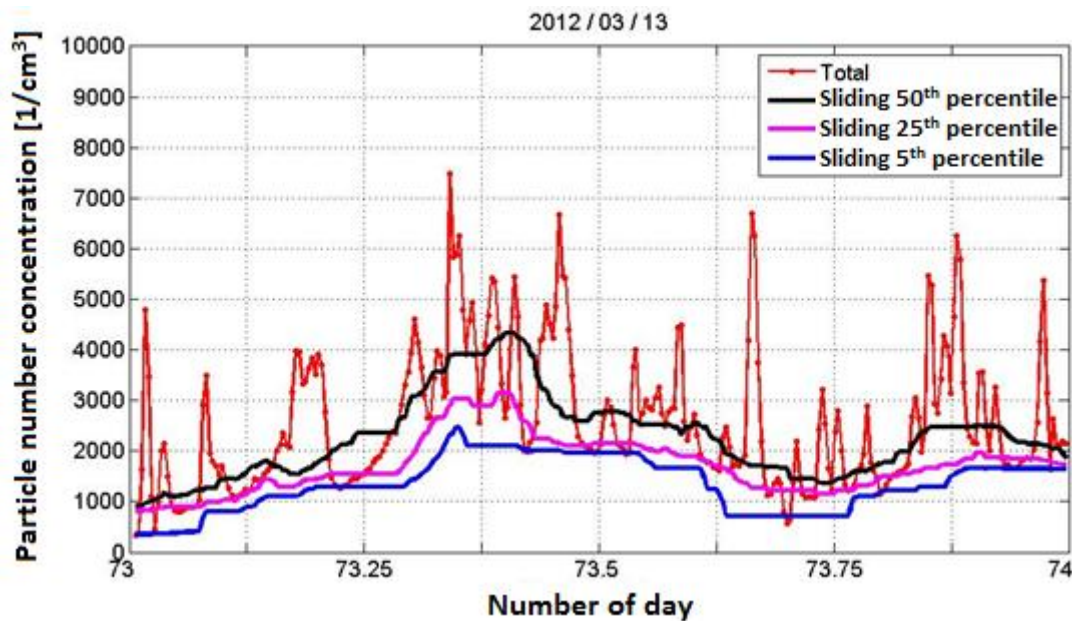


Figure 21. The red line shows the total concentration measured during March 13th, 2012. The blue, purple and black lines represent the 5th, 25th and 50th sliding percentiles, respectively.

Our results show that there are on average 9.3 plumes per day which would mean that about 9 ships per day were passing by on the ship lane daily. The real number is, however, on the order of 100 ships per day. This difference can be caused by many factors. We estimated the background particle concentrations over the sea from the data measured at Høvsøre and it is probable that the background particle concentration contains also the more dispersed ship plumes which do not appear as peaks in our measurement data. The smaller plumes that do not fulfill our plume criteria are also not included in the daily number of plumes. Notice however that they are not included in the background either. Hence, they do not contribute to raising the background concentration. Lowering the plume criteria would include more of the smaller plumes in the plume number and would contribute to the lower limit of the plume contribution (underestimation method), but would not affect the upper limit contribution values (overestimation method). Another factor is that some plumes can be combinations of plumes from two or more ships, but cannot be separated with our method. The average duration of a plume was 11 minutes, which gave us a total ship plume time around 100 min. If we assume that the real number of ship plumes was 100 (estimated and extrapolated to a whole day from *marinetraffic.com*) instead of 9.3, the total ship plume time would have been roughly 18 hours. This means that it is likely that a significant fraction of the particles in the estimated background concentration come from ships in our shipping lane. As a consequence, we might be underestimating the contribution from ships further away on the ship lane, or from ships that are emitting a lower number of particles.

The size distribution for the plume peak particles was mostly in the range between 30-60 nm. The average particle diameter was 41 nm in our measurements. This was larger compared to measurements by Jonsson et al. (2011). Their measurements were of fresh ship plumes, while particles in our plumes have been in the atmosphere for approximately an hour, allowing them to grow in size due to the process of condensation and coagulation. Also, the dilution and the dry deposition of the particles will take place during a longer time period and therefore result in a reduced concentration (Tian et al., 2013).

Our results indicate that a majority of the particles emitted by the ships are in the size ranges up to 100 nm. However, the peak of the solar spectrum is between 400-700 nm and in order

for the aerosol particles to effectively scatter sunlight the particles have to grow in size, which can take several days in the atmosphere. Only then can we state that these particles contribute to a reduced warming of the climate via scattering of sunlight. Particles with diameters smaller than 100 nm are already in the size range where they can act as CCN for cloud droplet formation moderating cloud properties. However, we do not know the extent of the reduced warming due to CCN particles from ship emissions since we do not know with certainty if these particles are hygroscopic or hydrophobic.

In the near future it might be interesting to connect observed plumes to individual ships using Ship Automatic Identification System (AIS) data. This would allow to separate different types of ships and to connect each individual ship to its position on a shipping lane. Regarding the shipping lane near Høvsøre, it could then be determined how far away from the route the ship is and what kind of emissions it is emitting.

Other aspects that could be analyzed are the meteorological conditions (especially PBL) and their effect on the observed plume- and background concentrations.

Overall we think that this model created for analyzing particle sizes and concentrations, is a good approximation of reality and is a good way to obtain results from other regions with a similar environment by applying this analysis method to other suitable locations.

Acknowledgements

We would like to thank our supervisors PhD. Adam Kristensson and Post Doc. Niku Kivekäs for their support and sharing of their knowledge with us. We are thankful for the guidance that we received during the work. We would also like to thank Adam and Niku for sharing the data from Høvsøre with us.

References

- Albrecht, B. A., Aerosols, cloud microphysics, and fractional cloudiness, *Science*, Vol. 245, p. 1227-1230, 1989
- Benson, D.R, et al., When does new particle formation not occur in the upper troposphere?, *Atmospheric Chemistry and Physics Discussions*, No. 7, 2007.
- Bolund, P. and Hunhammer, S., Ecosystem services in urban areas. *Ecological Economics*, Vol. 29, p. 293-301, 1999
- Bowker, G., et al., The effects of roadside structures on the transport and dispersion of ultrafine particles from highways. *Atmospheric Environment* 41, p. 8128-8139, 2007
- Corbett, J. et al., Mortality from Ship Emissions: A Global Assessment, *Science & Environmental Health Network*, 2007.
- Dal Maso, M. et al., Formation and growth of fresh atmospheric aerosols: eight years of aerosol size distribution data from SMEAR II, Hyytiälä, Finland, *Boreal environment research*, No. 10, p. 323–336, 2005.
- EEA Technical report, The impact of international shipping on European air quality and climate forcing, ISSN 1725-2237, No. 4, 2013
- Facchini, M. et al., Primary submicron marine aerosol dominated by insoluble organic colloids and aggregates, *Geophysical Research Letters*, vol. 35, p. 1-5, 2008.
- Genberg, J. et al., Source Apportionment of Carbonaceous Aerosol: Measurement and Model Evaluation, ISBN: 978-91-7473-428-7, 2013
- Grübler, A. et al., The Rise and Fall of Infrastructures, *Physica-Verlag Heidelberg*, p. 87, 1990.
- Hedberg, E., et al., Chemical and Physical Characterization of Emissions from Birch Wood Combustion in a Wood Stove, *Atmospheric Environment* 36, p. 4823–4837, 2002.
- Hedberg, E., et al., Is Levoglucosan a Suitable Quantitative Tracer for Wood Burning? Comparison with Receptor Modeling on Trace Elements in Lycksele, Sweden, *Journal of the Air & Waste Management Association*, Vol. 56, p. 1669–1678, 2006.
- Hussein, T., et al. Time span and spatial scale of regional new particle formation events over Finland and Southern Sweden. *Atmospheric Chemistry and Physics* 9, p. 4699–4716, 2009.
- IPCC, *Climate Change 2007: Synthesis Report*, ISSN 1725-2237, p. 36-41, 2007
- Janssen, N. A. H. et al., Black Carbon as an Additional Indicator of the Adverse Health Effects of Airborne Particles Compared with PM₁₀ and PM_{2.5}, *Environment Health Perspective*, Vol 119, Issue 12, 2011
- Johansson, C., et al. Spatial & temporal variations of PM₁₀ and particle number concentrations in urban air. *Environmental Monitoring and Assessment*, Vol. 127 p. 477–487, 2007
- Jonsson, Å. et al., Size-resolved particle emission factors for individual ships, *Geophysical Research Letters*, Vol. 38, Issue 13, p. 1-5, 2011
- Kirkham, P., Oxidative Stress and Macrophage Function: A Failure to Resolve the Inflammatory Response, *Biochemical Society Transactions*, Vol. 35, Pt. 2, p. 284-287, 2007

- Kittelson, D. B. Engines and nanoparticles: A review. *Journal of Aerosol Science*, 29, p. 575-588, 1998.
- Kivekäs, N., Aerosol size distribution and its connection to cloud droplet number concentration, Report series in aerosol science, No. 113, 2010
- Kreyling, W.G. et al., Ultrafine particle-lung interactions: does size matter?, *Journal of Aerosol Medicine*, Vol. 19, Issue 1, p. 74-83, 2006
- Kristensson, A. Aerosol Particle Sources Affecting the Swedish Air Quality at Urban and Rural Level, Doctoral Thesis, Division of Nuclear Physics, Department of Physics, Lund University, P. O. Box 118, SE-221 00, Lund, Sweden, ISBN 91-628-6573-0, 2005.
- Kristensson, A. et al., Partiklar i Malmöluften. Sammansättning, källor, hälsoeffekter, åtgärder., Malmö miljöförvaltning, Lund universitet, http://www.miljo.skane.se/sv/d/bilagor/Partiklar_Malmoluften.pdf, 2011
- Kulmala, M. et al., On the formation, growth and composition of nucleation mode particles, *Tellus*, ISSN: 0280–6509, 2001
- Kulmala, M. et al., Aerosol formation during PARFORCE: Ternary nucleation of H₂SO₄, NH₃ and H₂O. *Journal of Geophysical Research-Atmospheres* 107, 2002
- Kulmala, M. et al., Initial steps of aerosol growth, *Atmospheric Chemistry and Physics* 4, p. 2553-2560, 2004
- Kulmala, M., and Kerminen, V. M., On the formation and growth of atmospheric nanoparticles. *Atmospheric Research*, Vol. 90, Issue 2-4, p. 132-150, 2008
- Kulmala, M. et al., Direct Observations of Atmospheric Aerosol Nucleation, *Science* 339, Vol. 943, p. 943-946, 2013
- Löndahl, J. et al. Aerosol exposure versus aerosol cooling of climate: what is the optimal emission reduction strategy for human health?, *Atmospheric chemistry and physics*, Vol.10, 2010
- McPherson, E. et al., Quantifying urban forest structure, function, and value: the Chicago Urban Forest Climate Project, *Urban Ecosystems*, Vol. 1, p. 49-61, 1997
- Murray, C. et al., The world health report 2002 Reducing risks, promoting healthy life, World health organization, Geneva, 2002
- Nemmar, A. et al., Passage of Inhaled Particles Into the Blood Circulation in Humans, *Circulation*, Vol. 105, Issue 4, p. 411-414, 2002
- Nowak, D. et al., Air pollution removal by urban trees and shrubs in the United States, *Urban Forestry and Urban Greening*, Vol. 4, p. 115-123, 2006
- Oberdorster, G. et al., Translocation of Inhaled Ultrafine Particles to the Brain, *Inhalation Toxicology*, Vol. 16, p. 437-445, 2004
- Querol, X., et al., African dust contributions to mean ambient PM₁₀ mass-levels across the Mediterranean Basin, *Atmospheric Environment* 43, p. 4266–4277, 2009.
- Samoli, E. et al., Estimating the Exposure-Response Relationships Between Particulate Matter and Mortality Within the APHEA Multiplicity Project, *Environmental Health Perspectives*, Vol. 113, p. 88-95, 2005
- Seinfeld, J.H., and Pandis, S.N. *Atmospheric chemistry and physics; from air pollution to climate change*, Wiley-Interscience publication, Second edition, New Jersey, 2006, p.596

Slinn, W. et al., Predictions for particle deposition to vegetative canopies, *Atmospheric Environment*, Vol. 16, 1982.

Smith, L. and Stephenson, S. et al., New Trans-Arctic shipping routes navigable by midcentury, *PNAS Early edition*, p. 1-5., 2013

Squizzato, S. et al. Factors determining the formation of secondary inorganic aerosol: a case study in the Po Valley (Italy), *Atmospheric chemistry and physics*, Vol.13, 2013

Tian, J. et al., Modeling the evolution of aerosol particles in a ship plume using PartMC-MOSAIC, *Atmospheric Chemistry and Physics Discussions*, Vol. 13, p. 16733–16774, 2013

Twomey, S., The influence of pollution on the short wave albedo of clouds, *J. Atmos. Sci.*, vol. 34, pp. 1149–1152, 1977

Woodcock, J. et al., Public health benefits of strategies to reduce greenhouse-gas emissions: urban land transport, *The Lancet*, Vol. 374, Issue 9705, p. 1930-43, 2009

Zhou, J., *Hygroscopic Properties of Atmospheric Particles in Various Environments*, ISBN: 91-7874-120-3, 2001